Measuring the trilinear Higgs boson self-coupling at the 100 TeV hadron collider via multivariate analysis

Jubin Park,[1,2] Jung Chang,[2] Kingman Cheung,[3,4,5] and Jae Sik Lee[2,1]

[1]*IUEP, Chonnam National University, Gwangju 61186, Korea*
[2]*Department of Physics, Chonnam National University, Gwangju 61186, Korea*
[3]*Physics Division, National Center for Theoretical Sciences, Hsinchu 300, Taiwan*
[4]*Division of Quantum Phases and Devices, School of Physics, Konkuk University, Seoul 143-701, Republic of Korea*
[5]*Department of Physics, National Tsing Hua University, Hsinchu 300, Taiwan*

(Received 9 April 2020; accepted 10 September 2020; published 14 October 2020)

We perform a multivariate analysis of Higgs-pair production via the decay channel $HH \to b\bar{b}\gamma\gamma$ at the future 100 TeV pp collider to determine the trilinear Higgs self–coupling (THSC) λ_{3H}, which takes the value of 1 in the standard model. We consider all known background processes. For the signal we adopt the most recent event generator of POWHEG-BOX-V2 to exploit the NLO distributions for toolkit for multivariate data analysis (TMVA). Through the technique of boosted decision tree (BDT) analysis trained for $\lambda_{3H} = 1$, compared to the conventional cut-and-count approach, the signal-to-background ratio improves tremendously from about $1/10$ to 1 and the significance can reach up to 20.5 with a luminosity of 3 ab^{-1} without including systematic uncertainties. In addition, by implementing a likelihood fitting of the signal-plus-background $M_{\gamma\gamma bb}$ distribution with optimized bin sizes, it is possible to determine the THSC with the precision of 7.5% at 68% CL even at the early stage of 100 TeV hadron collider with 3 ab^{-1}.

DOI: 10.1103/PhysRevD.102.073002

I. INTRODUCTION

Since the discovery of the 125 GeV Higgs boson in 2012 at the LHC [1], we have been looking for a clear signal or even a hint of new physics beyond the Standard Model (SM) but without much success. Moreover, after completing the Runs I and II at the LHC, it turns out that the 125 GeV Higgs boson is best described as the SM Higgs boson [2], although there is an upward trend in the overall signal strength [3]. Under this situation, one of the most solid avenues to explore for new physics is to measure the Higgs potential which could be significantly different from that of the SM.

Higgs-boson pair production at the high-luminosity and/or high-energy hadron colliders provides a very useful way to probe the Higgs potential via the investigation of the trilinear Higgs self-coupling (THSC) [4–6]. The specific decay modes considered are: $b\bar{b}b\bar{b}$ [7], $b\bar{b}\gamma\gamma$ [8,9], $b\bar{b}\tau^+\tau^-$ [10], $b\bar{b}W^+W^-$ [11], and some combinations of these channels [12,13]. Higgs-boson pair production also has been vastly studied in models beyond the SM [14].

The current limits on the THSC in units of λ_{3H}, which takes the value of 1 in the SM, are $-5.0 < \lambda_{3H} < 12$ from ATLAS [15] and $-11.8 < \lambda_{3H} < 18.8$ from CMS [16] at 95% confidence level (CL). At the high-luminosity option of the LHC running at 14 TeV (HL-LHC) with an integrated luminosity of 3 ab^{-1}, a combined ATLAS and CMS projection of the 68% CL interval is $0.57 < \lambda_{3H} < 1.5$ without including systematic uncertainties [17]. On the other hand, at the International Linear Collider (ILC) operated at 1 TeV can reach the precision of 10% at 68% CL with an integrated luminosity of 8 ab^{-1} [18,19].

In this work, we perform a multivariate analysis of Higgs-pair production in $HH \to b\bar{b}\gamma\gamma$ channel at the 100 TeV hadron collider. In our previous work, based on the conventional cut-and-count analysis, it was shown that the THSC can be measured with about 20% accuracy at the SM value with a luminosity of 3 ab^{-1} [20]. In this paper, with the use of the BDT method closely following Ref. [21], we show that the THSC can be measured with a precision of 7.5% at 68% CL at the 100 TeV hadron collider assuming 3 ab^{-1} luminosity, which is superior to the accuracy expected at the 1 TeV ILC even with 8 ab^{-1}.

II. EVENT GENERATION AND TMVA ANALYSIS

The Higgs bosons in the signal event samples are generated on-shell with a zero width by POWHEG-BOX-V2

TABLE I. Monte Carlo samples used in Higgs-pair production analysis $H(\to b\bar{b})H(\to \gamma\gamma)$, and the corresponding codes for the matrix-element generation. PYTHIA8 is used for parton showering and hadronization. We refer to Ref. [33] for MG5_aMC@NLO.

Signal					
Signal process		Generator	$\sigma \cdot BR$ [fb]	Order in QCD	PDF used
$gg \to HH \to b\bar{b}\gamma\gamma$		POWHEG-BOX-V2	3.25	NNLO	PDF4LHC15_nlo
Backgrounds					
Background(BG)	Process	Generator	$\sigma \cdot BR$ [fb]	Order in QCD	PDF used
Single-Higgs associated BG	$ggH(\to \gamma\gamma)$	POWHEG-BOX	1.82×10^3	NNNLO	CT10
	$t\bar{t}H(\to \gamma\gamma)$	PYTHIA8	7.29×10^1	NLO	
	$ZH(\to \gamma\gamma)$	PYTHIA8	2.54×10^1	NNLO	
	$b\bar{b}H(\to \gamma\gamma)$	PYTHIA8	1.96×10^1	NNLO(5FS)	
Non-resonant BG	$b\bar{b}\gamma\gamma$	MG5_aMC@NLO	2.28×10^3	LO	CT14LO
	$c\bar{c}\gamma\gamma$	MG5_aMC@NLO	1.92×10^4	LO	MLM [29,30]
	$jj\gamma\gamma$	MG5_aMC@NLO	4.20×10^5	LO	
	$b\bar{b}j\gamma$	MG5_aMC@NLO	0.96×10^7	LO	
	$c\bar{c}j\gamma$	MG5_aMC@NLO	3.19×10^7	LO	CT14LO
	$b\bar{b}jj$	MG5_aMC@NLO	1.00×10^{10}	LO	Refs. [9,13,20]
	$Z(\to b\bar{b})\gamma\gamma$	MG5_aMC@NLO	7.87×10^1)	LO	
$t\bar{t}$ and $t\bar{t}\gamma$ BG ($\geq$1 lepton)	$t\bar{t}$	MG5_aMC@NLO	1.76×10^7	NLO	CT10
	$t\bar{t}\gamma$	MG5_aMC@NLO	4.18×10^4	NLO	CTEQ6L1

[22,23] with the damping factor hdamp set to the default value of 250 to limit the amount of hard radiation. This code provides NLO distributions matched to a parton shower taking account of the full top-quark mass dependence. The signal cross section at NNLO order in QCD is calculated according to $\sigma^{\rm NNLO}(\lambda_{3H}) = K_{\rm SM}^{\rm NNLO/NLO} \times \sigma^{\rm NLO}(\lambda_{3H})$ using $\sigma^{\rm NLO}(\lambda_{3H})$ from POWHEG-BOX-V2 and $K_{\rm SM}^{\rm NNLO/NLO} = 1.067$ [24][1] in the FT approximation in which the full top-quark mass dependence is considered only in the real radiation while the Born improved Higgs effective field theory is taken in the virtual part. And then, the MadSpin code [26] is used for the decay of both Higgs bosons into two bottom quarks and two photons.

For generation and simulation of backgrounds, we closely follow Ref. [20],[2] except for the use of the post-LHC PDF set of CT14LO [28] for nonresonant backgrounds. Furthermore, for the two main nonresonant backgrounds of $b\bar{b}\gamma\gamma$ and $c\bar{c}\gamma\gamma$, we use the merged cross sections and distributions by MLM matching [29,30] with xqcut and $Q_{\rm cut}$ set to 20 GeV and 30 GeV, respectively. For the remaining nonresonant backgrounds, we are using the cross sections and distributions obtained by applying the generator-level cuts as adopted in Ref. [9,13] which might provide more reliable and conservative estimation of the nonresonant backgrounds containing light jets [20].

For parton showering and hadronization, PYTHIA8 [31] is used both for signal and backgrounds. Finally, fast-detector simulation and analysis are performed using DELPHES3 [32] with the DELPHES-FCC template.

All the signal and backgrounds are summarized in Table I, together with information of the corresponding event generator, the cross section times the branching ratio and the order in QCD, and the parton distribution function (PDF) used.

A multivariate analysis is performed using TMVA [34] with ROOTv6.18 [35]. After applying a sequence of event selections as in Table II, we choose the following 8 kinematic variables for TMVA:

TABLE II. Sequence of event selection criteria applied in this analysis.

Sequence	Event Selection Criteria at the 100 TeV hadron collider
1	Diphoton trigger condition, ≥ 2 isolated photons with $P_T > 30$ GeV, $\lvert\eta\rvert < 5$
2	≥ 2 isolated photons with $P_T > 40$ GeV, $\lvert\eta\rvert < 3$, $\Delta R_{j\gamma,\gamma\gamma} > 0.4$
3	≥ 2 jets identified as b-jets with leading(subleading) $P_T > 50(40)$ GeV, $\lvert\eta\rvert < 3$, $\Delta R_{bb} > 0.4$
4	Events are required to contain ≤ 5 jets with $P_T > 40$ GeV within $\lvert\eta\rvert < 5$
5	No isolated leptons with $P_T > 40$ GeV, $\lvert\eta\rvert < 3$
6	TMVA analysis

[1]According to the recent N3LO calculations [25], the signal cross section is further enhanced by the amount of 2.7% which would hardly affect our conclusion, or rather strengthen our results.

[2]Specifically, the multivariate MV1 b-tagging algorithm with $\epsilon_b = 0.75$ is taken together with $P_{c\to b} = 0.1$, $P_{j\to b} = 0.01$, and $P_{j\to\gamma} = 1.35 \times 10^{-3}$ [27].

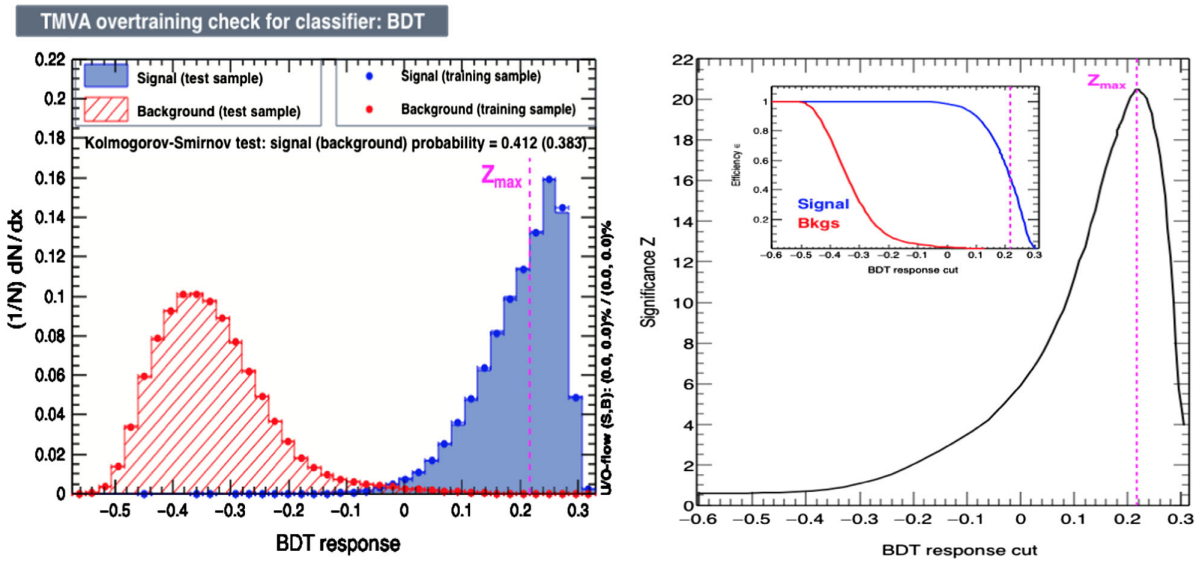

FIG. 1. (Left) Normalized SM BDT responses for test (histogram) and training (dots with error bars) samples. BDT responses for signal (blue) and background (red) samples, which mostly populate in the regions with positive and negative BDT response, respectively. (Right) Signal and background efficiencies (inset) and significance Z as functions of BDT response cut. $\mathrm{BDT_{SM}}$ is used. The vertical lines show the position of the optimal cut on the BDT response which maximizes the significance.

$$M_{bb},\quad P_T^{bb},\quad \Delta R_{bb};\quad M_{\gamma\gamma},\quad P_T^{\gamma\gamma},\quad \Delta R_{\gamma\gamma};\quad M_{\gamma\gamma bb},\quad \Delta R_{\gamma b}.$$

The judicious choice of the two photons or two b quarks for the above TMVA variables has been made as in [21]. We also refer to Ref. [21] for the details of our TMVA setup and analysis. And we choose BDT for our analysis since the BDT-related methods show higher performance with better signal efficiency and stronger background rejection.

III. RESULTS

In the left panel of Fig. 1, we show the BDT responses obtained using BDT trained for $\lambda_{3H} = 1$ which is dubbed as $\mathrm{BDT_{SM}}$. By validating the BDT distributions for the training sample (dots with error bars) with those for the test sample (histogram), we check that $\mathrm{BDT_{SM}}$ is not overtrained. In the right panel of Fig. 1, using $\mathrm{BDT_{SM}}$, we show the behavior of signal and background efficiencies (inset) and significance $Z = \sqrt{2\cdot[((s+b)\cdot\ln(1+s/b)-s)]}$ with s and b being the numbers of signal and background events as functions of the cut value on BDT response. The significance can reach up to 20.50 when the BDT response is cut at 0.216, at which, the signal and background efficiencies are 0.48 and 1.58×10^{-4}, respectively. We denote by vertical lines the positions of the optimal cut on the BDT response which maximizes the significance.

In Table III, we present the expected number of signal and background events at the 100 TeV hadron collider assuming 3 $\mathrm{ab^{-1}}$ using $\mathrm{BDT_{SM}}$ with the BDT response cut of 0.216. We show the four representative values of λ_{3H} for signal and the backgrounds are separated into three categories. For comparisons, we also show the results obtained using the cut-and-count analysis [20]. In the last column, we additionally present the effective luminosity (Eff. Lumi.) for each of signal and background samples. In the $t\bar{t}$ and $t\bar{t}\gamma$ backgrounds, the first (second) number is the effective luminosity when the two top quarks decay fully (semi-) leptonically. We find about 550 signal and 550 background events for $\lambda_{3H} = 1$. Comparing to the results using the cut-and-count analysis [20], the number of signal events decreases by only 19% while the number of backgrounds by almost 90%, resulting in an increase in significance from 8.44 to 20.50. Note that the composition of backgrounds changes drastically by the use of BDT. In the cut-and-count analysis, the nonresonant background is about two times larger than the single-Higgs associated background. While, in the BDT analysis, the single-Higgs associated background is more than four times larger than the nonresonant one and $t\bar{t}$ associated background becomes negligible. Note that we generate relatively smaller number of events for the $c\bar{c}\gamma\gamma$, $c\bar{c}j\gamma$, and $b\bar{b}jj$ backgrounds since we observe that they quickly decrease when the BDT response cut approaches to the point $Z_{\max}$ of 0.216.[3] Specifically, the $b\bar{b}jj$ background vanishes for the BDT response cut larger than 0.2. Otherwise, we generate enough number of events considering the assumed luminosity of 3 $\mathrm{ab^{-1}}$.

First, we try to determine the THSC considering the total number of events. As shown in the left panel of Fig. 2, we

[3]In fact, there are some differences in kinematic distributions among the non-resonant backgrounds. For example, the $c\bar{c}\gamma\gamma$ background is more populated in the region of $\Delta R_{bb} > 3$ compared to the $b\bar{b}\gamma\gamma$ one.

TABLE III. Expected number of signal and background events at the 100 TeV hadron collider assuming 3 ab^{-1} using BDT$_{SM}$ with the BDT response cut of 0.216. See text for explanation.

	Expected yields (3 ab^{-1})			
Signal and Backgrounds	Pre-Selection	BDT$_{SM}$	Cut-and-Count	Eff. Lumi. (ab^{-1})
$H(b\bar{b})H(\gamma\gamma)$, $\lambda_{3H}=-3$	7253.98	2408.37	3400.08	10.7
$H(b\bar{b})H(\gamma\gamma)$, $\lambda_{3H}=0$	2072.09	902.49	1146.21	44.5
$\mathbf{H(b\bar{b})H(\gamma\gamma)}$, $\boldsymbol{\lambda_{3H}=1}$	**1124.48**	**548.02**	**673.29**	**615**
$H(b\bar{b})H(\gamma\gamma)$, $\lambda_{3H}=5$	1480.24	251.13	439.29	40.9
$ggH(\gamma\gamma)$	5827.41	255.86	875.71	17.0
$t\bar{t}H(\gamma\gamma)$	11371.21	145.88	868.73	13.2
$ZH(\gamma\gamma)$	593.29	38.88	168.86	39.4
$b\bar{b}H(\gamma\gamma)$	205.45	2.59	9.82	51.0
$b\bar{b}\gamma\gamma$	183493.56	55.01	336.49	19.2
$c\bar{c}\gamma\gamma$	66600.78	0.00	54.66	0.11
$jj\gamma\gamma$	14182.56	2.52	25.20	2.38
$b\bar{b}j\gamma$	1228956.91	38.53	1176.93	3.74
$c\bar{c}j\gamma$	208285.83	0.00	187.92	0.26
$b\bar{b}jj$	1622778.23	0.00	2231.08	0.19
$Z(b\bar{b})\gamma\gamma$	4540.20	4.72	45.33	12.7
$t\bar{t}$ ($\geq$1 leptons)	78490.03	0.00	56.93	$11.5+3.68$
$t\bar{t}\gamma$ ($\geq$1 leptons)	74885.54	9.09	105.16	$8.69+2.07$
Total Background	3500211.00	553.09	6142.83	
Significance Z, $\lambda_{3H}=1$		**20.50**	**8.44**	

find that the THSC can be measured with about 11% accuracy at the SM value which is about two times better than the result based on the conventional cut-and-count analysis [20]. However, there is a second solution around $\lambda_{3H}=6.5$. To lift up the two-fold ambiguity, we implement a likelihood fitting of the signal-plus-background $M_{\gamma\gamma bb}$ distribution and find the second solution is ruled out by more than 8σ confidence, see the right panel of Fig. 2.

To improve the sensitivity of the THSC around the SM value and to tame the statistical fluctuation due to the limited size of the MC samples, we repeat the likelihood fitting of $M_{\gamma\gamma bb}$ distribution by optimizing the bin size

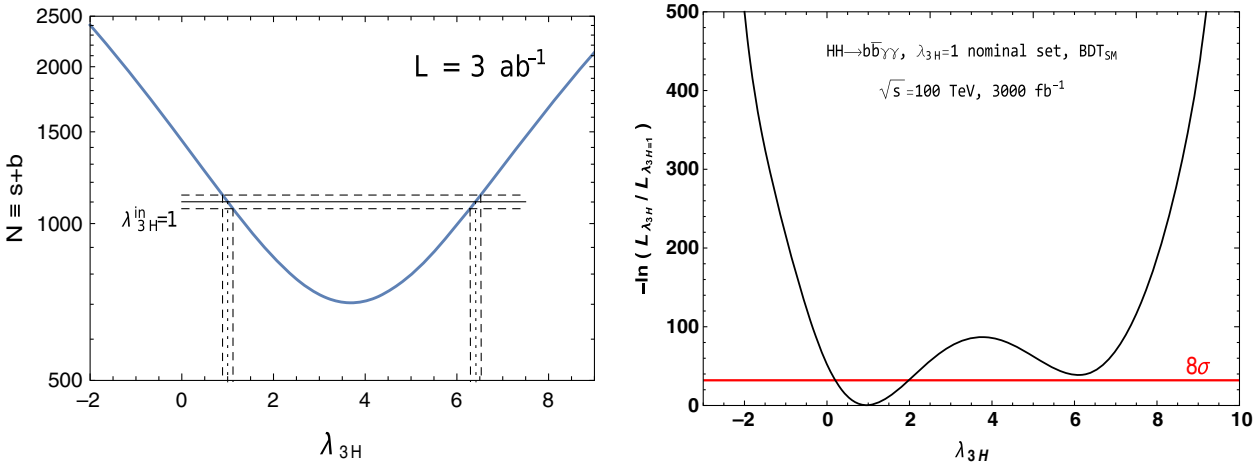

FIG. 2. (Left) The total number $N=s+b$ of signal (s) and background (b) events versus λ_{3H} with 3 ab^{-1}. The horizontal solid line denotes the total number of events obtained using the SM value of $\lambda_{3H}=1$ and the dashed lines for the statistical 1-σ error. (Right) The relative log likelihood distribution for the nominal value of $\lambda_{3H}=1$ at the 100 TeV hadron collider assuming 3 ab^{-1} and using BDT$_{SM}$ with the BDT response cut of 0.216. The distribution has been obtained by a likelihood fitting of $M_{\gamma\gamma bb}$ distribution for each value of λ_{3H}. The black solid line shows the result of a polynomial fitting and the horizontal solid (red) line at $-\ln(L_{\lambda_{3H}}/L_{\lambda_{3H}=1})=32$ indicates the value corresponding to the 8σ level.

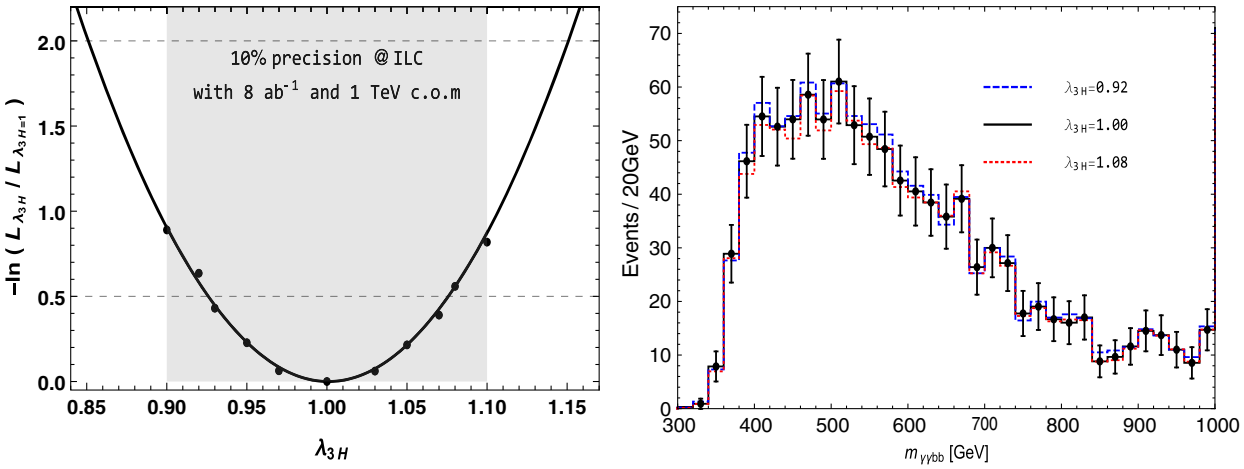

FIG. 3. Left: the relative log likelihood distribution for the nominal value of $\lambda_{3H} = 1$ at the 100 TeV hadron collider with 3 ab^{-1}. The black circles are the values obtained by a likelihood fitting of $M_{\gamma\gamma bb}$ distributions using $\mathrm{BDT_{SM}}$ with the BDT response cut of 0.216. The black solid line shows the result of a polynomial fitting and the thin dashed line at 0.5(2.0) indicates the value corresponding to a $1\sigma(2\sigma)$ CI. The shaded region shows the 1σ CI expected at the ILC at 1 TeV with 8 ab^{-1}. Right: the SM $M_{\gamma\gamma bb}$ distribution (solid line with dots with 1σ error bars) and those for $\lambda_{3H} = 0.92$ and 1.08 (dashed lines).

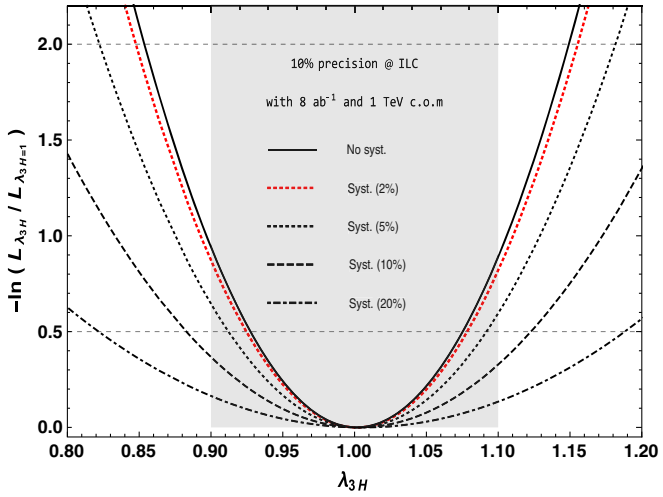

FIG. 4. The same as in the left panel of Fig. 3 while taking $\sigma_b/b = 0$ (solid), 0.02 (red dotted) 0.05 (black dotted), 0.1 (dashed), and 0.2 (dash-dotted).

between 1/20 GeV and 1/60 GeV. Finally, we find that the THSC can be determined with a precision of 7.5% at 68% CL as shown in the left panel of Fig. 3. In the right panel of Fig. 3, $M_{\gamma\gamma bb}$ distributions are shown for the THSC at the SM value and for the two values deviated by 1σ.

By now, we have considered only the statistical uncertainties which may eventually dominate the total uncertainties. Before concluding, we would like to discuss the effects of systematic uncertainties which could be important at the early stage of 100 TeV hadron collider. The systematic uncertainties might be taken into account by considering the variance of background σ_b^2 [36]. In this case, the error due to systematic uncertainties is proportional to the number of background or $\sigma_b \propto b$. We find that the THSC precision of 7.5%–18% at 68% CL while varying σ_b/b between 0 and 0.2, see Fig. 4.[4]

Finally, before we end this section, in Table IV, we show the relative importance of the variables that we employed in this BDT analysis. We observe that the two most important variables are ΔR_{bb} and $\Delta R_{\gamma\gamma}$, which is consistent with our previous cut-and-count analysis [20].

TABLE IV. The ranking of the variables that we employed in this BDT analysis in the descending order of importance.

ΔR_{bb}	$\Delta R_{\gamma\gamma}$	$M_{\gamma\gamma}$	$\Delta R_{\gamma b}$	$P_T^{\gamma\gamma}$	$M_{\gamma\gamma bb}$	P_T^{bb}	M_{bb}
0.163	0.152	0.150	0.133	0.110	0.102	0.096	0.095

IV. CONCLUSIONS

Higgs-pair production is one of the most useful avenue to probe the EWSB sector. We have studied in great details, with the help of machine learning, the sensitivity of measuring the THSC λ_{3H} that one can expect at the 100 TeV pp collider with an integrated luminosity 3 ab^{-1}. With TMVA one can improve the signal-to-background ratio for $\lambda_{3H} = 1$ to 1∶1 compared with the ratio 1∶10 obtained in the conventional cut-and-count approach. Furthermore, the significance of such a signal jumps to 20.

Other than determining the THSC by measuring the total number of events, one can also improve the sensitivity and lift the two-fold degeneracy by implementing a likelihood fitting of the signal-plus-background $M_{\gamma\gamma bb}$ distribution with optimized bin sizes. The THSC can be determined

[4]Incidentally, by measuring only the total number of events, the precision becomes worse to 11%–30%.

with a precision of 7.5% at 68% CL with 3 ab^{-1}, which is indeed better than the ILC running at 1 TeV with 8 ab^{-1}. Extrapolating our result conservatively, we expect that one can achieve the precision better than ~2% with 30 ab^{-1}.

ACKNOWLEDGMENTS

This work was supported by the National Research Foundation of Korea Grant No. NRF-2016R1E1A1A01943297 (J. C., J. S. L., J. P.), No. NRF-2018R1D1A1B07051126 (J. P.), and by the MoST of Taiwan under Grant No. 107-2112-M-007-029-MY3 (K. C.).

Note added.—After the completion of our work, we learned a similar analysis performed considering various systematic uncertainties rigorously [37]. They found the combined precision of 2.9%–5.5% with 30 ab^{-1} at 68% CL which is in a good quantitative agreement with our results.

APPENDIX: EXTRAPOLATION OF BDT CUTS

For this work, we generate relatively smaller number of events for the $c\bar{c}\gamma\gamma$, $c\bar{c}j\gamma$, and $b\bar{b}jj$ backgrounds which may lead to underestimation of the relevant backgrounds.

The $c\bar{c}\gamma\gamma$ and $c\bar{c}j\gamma$ backgrounds might be negligible since, taking account of the fake rates $P_{c\to b}$ and $P_{j\to\gamma}$, the cross sections are smaller than that of the $b\bar{b}\gamma\gamma$ background by about an order of magnitude. On the other hand, our estimation of the $b\bar{b}jj$ background could be unreliable due to the limited size of the MC sample. Here we try to estimate the background yield based on the current sample.

Precisely, we study the behavior of the $b\bar{b}jj$ background yield $Y_{b\bar{b}jj}$ versus the BDT response cut. First we observe that, based on the current $b\bar{b}jj$ MC sample, our estimation of the background results in 0 when BDT Cut > 0.19, see the upper-left panel of Fig. 5. To extrapolate to the region with BDT Cut > 0.19, we implement a linear fitting to $\log Y_{b\bar{b}jj}$, see the solid line in the upper-right panel of Fig. 5. And we find that

$$Y_{b\bar{b}jj} = 13.7^{+2.2(5.2)}_{-1.9(3.7)} \tag{A1}$$

at 68(95)% CL as shown in the lower panel of Fig. 5. Taking the 1σ upper value of 15.9, the number of total background increases by the amount of about 3% which hardly affects our main results significantly.

Incidentally, we note that the $jj\gamma\gamma$ background survives though its cross section is smaller than that of the $b\bar{b}\gamma\gamma$ one

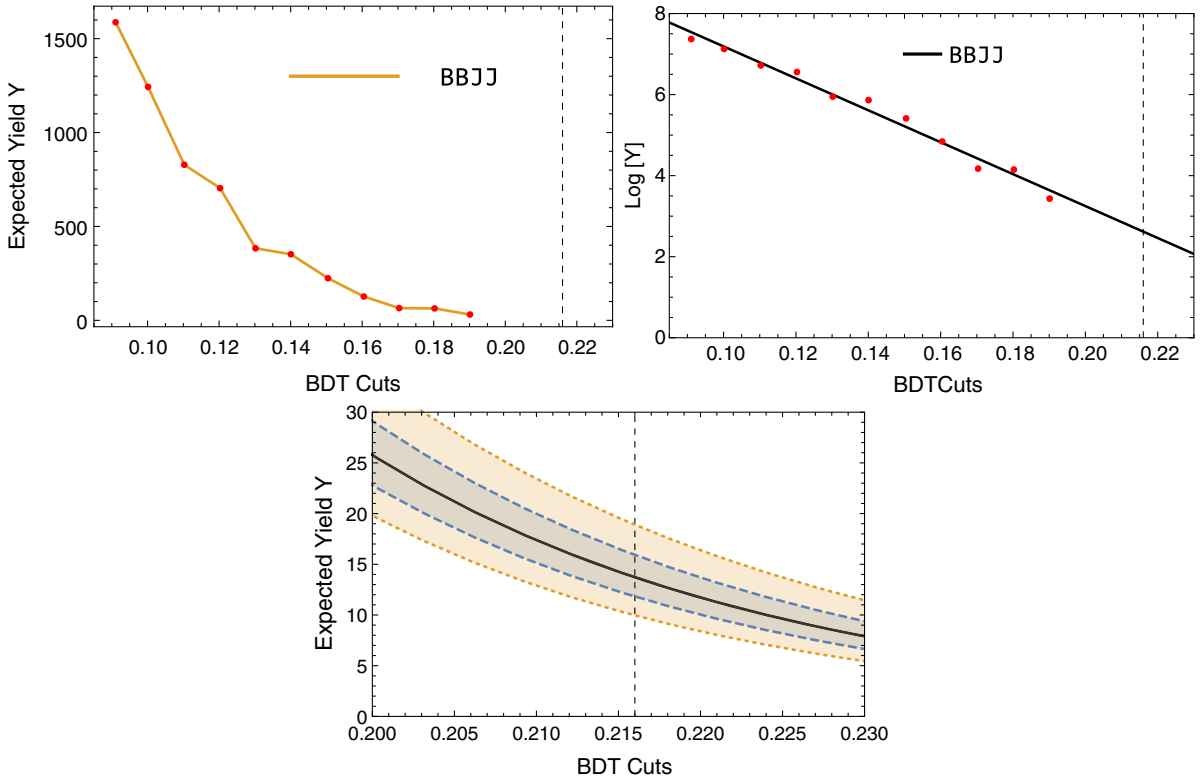

FIG. 5. Behavior of the $b\bar{b}jj$ background yield $Y_{b\bar{b}jj}$ versus the BDT response cut. In the upper panels, the MC data points are denoted by bullets and the solid line in the upper-right panel shows the result of the linear fitting to $\log Y_{b\bar{b}jj}$. In the lower panel, we show the result of extrapolation of the solid line to the region with BDT Cut > 0.19, where no data points exist, together with 1- and 2-σ errors. The vertical lines locate the BDT response cut of 0.216 taken for $\mathrm{BDT_{SM}}$.

by about *two* orders of magnitude taking account of the fake rate $P_{j\to b}$. This is because its kinematical distributions quite resemble to those of the signal. For example, compared to other non-resonant backgrounds, we find that it is quite populated in the region of $\Delta R_{bb} \lesssim 2$ where most signal events located.

[1] G. Aad *et al.* (ATLAS Collaboration), Observation of a new particle in the search for the Standard Model Higgs boson with the ATLAS detector at the LHC, Phys. Lett. B **716**, 1 (2012); S. Chatrchyan *et al.* (CMS Collaboration), Observation of a new boson at a mass of 125 GeV with the CMS experiment at the LHC, Phys. Lett. B **716**, 30 (2012).

[2] K. Cheung, J. S. Lee, and P. Y. Tseng, Higgs precision (Higgcision) era begins, J. High Energy Phys. 05 (2013) 134; Higgs precision analysis updates 2014, Phys. Rev. D **90**, 095009 (2014).

[3] K. Cheung, J. S. Lee, and P. Y. Tseng, New emerging results in Higgs precision analysis updates 2018 after establishment of third-generation Yukawa couplings, J. High Energy Phys. 09 (2019) 098.

[4] E. W. N. Glover and J. J. van der Bij, Higgs Boson pair production via gluon fusion, Nucl. Phys. **B309**, 282 (1988); D. A. Dicus, C. Kao, and S. S. D. Willenbrock, Higgs boson pair production from gluon fusion, Phys. Lett. B **203**, 457 (1988); T. Plehn, M. Spira, and P. M. Zerwas, Pair production of neutral Higgs particles in gluon-gluon collisions, Nucl. Phys. **B479**, 46 (1996); Erratum, Nucl. Phys. **B531**, 655 (1998); A. Djouadi, W. Kilian, M. Muhlleitner, and P. M. Zerwas, Production of neutral Higgs boson pairs at LHC, Eur. Phys. J. C **10**, 45 (1999); S. Dawson, S. Dittmaier, and M. Spira, Neutral Higgs boson pair production at hadron colliders: QCD corrections, Phys. Rev. D **58**, 115012 (1998); U. Baur, T. Plehn, and D. L. Rainwater, Determining the Higgs boson self-coupling at hadron colliders, Phys. Rev. D **67**, 033003 (2003); T. Binoth, S. Karg, N. Kauer, and R. Ruckl, Multi-Higgs boson production in the Standard Model and beyond, Phys. Rev. D **74**, 113008 (2006);

[5] J. Baglio, A. Djouadi, R. Grber, M. M. Mhlleitner, J. Quevillon, and M. Spira, The measurement of the Higgs self-coupling at the LHC: Theoretical status, J. High Energy Phys. 04 (2013) 151; J. Cao, Z. Heng, L. Shang, P. Wan, and J. M. Yang, Pair Production of a 125 GeV Higgs Boson in MSSM and NMSSM at the LHC, J. High Energy Phys. 04 (2013) 134; D. de Florian and J. Mazzitelli, Two-loop virtual corrections to Higgs pair production, Phys. Lett. B **724**, 306 (2013); J. Grigo, J. Hoff, K. Melnikov, and M. Steinhauser, On the Higgs boson pair production at the LHC, Nucl. Phys. **B875**, 1 (2013); D. T. Nhung, M. Muhlleitner, J. Streicher, and K. Walz, Higher order corrections to the trilinear Higgs self-couplings in the real NMSSM, J. High Energy Phys. 11 (2013) 181; U. Ellwanger, Higgs pair production in the NMSSM at the LHC, J. High Energy Phys. 08 (2013) 077.

[6] E. Asakawa, D. Harada, S. Kanemura, Y. Okada, and K. Tsumura, Higgs boson pair production in new physics models at hadron, lepton, and photon colliders, Phys. Rev. D **82**, 115002 (2010); R. Contino, M. Ghezzi, M. Moretti, G. Panico, F. Piccinini, and A. Wulzer, Anomalous couplings in double Higgs production, J. High Energy Phys. 08 (2012) 154; G. D. Kribs and A. Martin, Enhanced di-Higgs production through light colored scalars, Phys. Rev. D **86**, 095023 (2012); S. Dawson, E. Furlan, and I. Lewis, Unravelling an extended quark sector through multiple Higgs production?, Phys. Rev. D **87**, 014007 (2013); M. J. Dolan, C. Englert, and M. Spannowsky, New Physics in LHC Higgs boson pair production, Phys. Rev. D **87**, 055002 (2013); M. Gouzevitch, A. Oliveira, J. Rojo, R. Rosenfeld, G. P. Salam, and V. Sanz, Scale-invariant resonance tagging in multijet events and new physics in Higgs pair production, J. High Energy Phys. 07 (2013) 148; R. S. Gupta, H. Rzehak, and J. D. Wells, How well do we need to measure the Higgs boson mass and self-coupling?, Phys. Rev. D **88**, 055024 (2013);

[7] U. Baur, T. Plehn, and D. L. Rainwater, Examining the Higgs boson potential at lepton and hadron colliders: A comparative analysis, Phys. Rev. D **68**, 033001 (2003); D. E. Ferreira de Lima, A. Papaefstathiou and M. Spannowsky, Standard model Higgs boson pair production in the $(b\bar{b})$ $(b\bar{b})$ final state, J. High Energy Phys. 08 (2014) 030; C. Englert, F. Krauss, M. Spannowsky, and J. Thompson, Di-Higgs phenomenology in $t\bar{t}hh$: The forgotten channel, Phys. Lett. B **743**, 93 (2015); T. Liu and H. Zhang, Measuring Di-Higgs Physics via the $t\bar{t}hh \to t\bar{t}b\bar{b}b\bar{b}$ Channel, arXiv:1410.1855; J. K. Behr, D. Bortoletto, J. A. Frost, N. P. Hartland, C. Issever, and J. Rojo, Boosting Higgs pair production in the $b\bar{b}b\bar{b}$ final state with multivariate techniques, Eur. Phys. J. C **76**, 386 (2016); F. Bishara, R. Contino, and J. Rojo, Higgs pair production in vector-boson fusion at the LHC and beyond, Eur. Phys. J. C **77**, 481 (2017).

[8] U. Baur, T. Plehn, and D. L. Rainwater, Measuring the Higgs Boson Self Coupling at the LHC and Finite Top Mass Matrix Elements, Phys. Rev. Lett. **89**, 151801 (2002); U. Baur, T. Plehn, and D. L. Rainwater, Probing the Higgs self-coupling at hadron colliders using rare decays, Phys. Rev. D **69**, 053004 (2004); V. Barger, L. L. Everett, C. B. Jackson, and G. Shaughnessy, Higgs-pair production and measurement of the triscalar coupling at LHC(8,14), Phys. Lett. B **728**, 433 (2014); W. Yao, Studies of measuring Higgs self-coupling with $HH \to b\bar{b}\gamma\gamma$ at the future hadron colliders, arXiv:1308.6302; Prospects for measuring Higgs pair production in the channel $H(\to \gamma\gamma)H(\to b\bar{b})$ using the ATLAS detector at the HL-LHC, Report No. ATL-PHYS-PUB-2014-019; A. J. Barr, M. J. Dolan, C. Englert, D. E. Ferreira de Lima, and M. Spannowsky, Higgs self-coupling measurements at a 100 TeV hadron collider, J. High Energy

Phys. 02 (2015) 016; A. Azatov, R. Contino, G. Panico, and M. Son, Effective field theory analysis of double Higgs boson production via gluon fusion, Phys. Rev. D **92**, 035001 (2015); A. Alves, T. Ghosh, and K. Sinha, Can we discover double Higgs production at the LHC?, Phys. Rev. D **96**, 035022 (2017); D. Gonalves, T. Han, F. Kling, T. Plehn, and M. Takeuchi, Higgs boson pair production at future hadron colliders: From kinematics to dynamics, Phys. Rev. D **97**, 113004 (2018); S. Homiller and P. Meade, Measurement of the triple Higgs coupling at a HE-LHC, J. High Energy Phys. 03 (2019) 055.

[9] ATLAS Collaboration, Study of the double Higgs production channel H(→ bb)H(→ gamma gamma) with the ATLAS experiment at the HL-LHC, Report No. ATL-PHYS-PUB-2017-001, 2017, http://cds.cern.ch/record/2243387.

[10] A. J. Barr, M. J. Dolan, C. Englert, and M. Spannowsky, Di-Higgs final states augMT2ed—selecting hh events at the high luminosity LHC, Phys. Lett. B **728**, 308 (2014); M. J. Dolan, C. Englert, N. Greiner, and M. Spannowsky, Further on Up the Road: $hhjj$ Production at the LHC, Phys. Rev. Lett. **112**, 101802 (2014).

[11] A. Papaefstathiou, L. L. Yang, and J. Zurita, Higgs boson pair production at the LHC in the $b\bar{b}W^+W^-$ channel, Phys. Rev. D **87**, 011301 (2013); V. Martn Lozano, J. M. Moreno, and C. B. Park, Resonant Higgs boson pair production in the $hh \to b\bar{b}WW \to b\bar{b}\ell^+\nu\ell^-\bar{\nu}$ decay channel, J. High Energy Phys. 08 (2015) 004.

[12] M. J. Dolan, C. Englert, and M. Spannowsky, Higgs self-coupling measurements at the LHC, J. High Energy Phys. 10 (2012) 112; F. Goertz, A. Papaefstathiou, L. L. Yang, and J. Zurita, Higgs Boson self-coupling measurements using ratios of cross sections, J. High Energy Phys. 06 (2013) 016; M. J. Dolan, C. Englert, N. Greiner, K. Nordstrom, and M. Spannowsky, $hhjj$ production at the LHC, Eur. Phys. J. C **75**, 387 (2015); A. Adhikary, S. Banerjee, R. K. Barman, B. Bhattacherjee, and S. Niyogi, Revisiting the non-resonant Higgs pair production at the HL-LHC, J. High Energy Phys. 07 (2018) 116; S. Banerjee, C. Englert, M. L. Mangano, M. Selvaggi, and M. Spannowsky, $hh+$jet production at 100 TeV, Eur. Phys. J. C **78**, 322 (2018); J. H. Kim, M. Kim, K. Kong, K. T. Matchev, and M. Park, Portraying double Higgs at the large hadron collider, J. High Energy Phys. 09 (2019) 047.

[13] ATLAS Collaboration, Measurement prospects of the pair production and self–coupling of the HIggs boson with the ATLAS experiment at the HL–LHC, Report No. ATL-PHYS-PUB-2018-053.

[14] C. O. Dib, R. Rosenfeld, and A. Zerwekh, Double Higgs production and quadratic divergence cancellation in little Higgs models with T parity, J. High Energy Phys. 05 (2006) 074; A. Arhrib, R. Benbrik, C. H. Chen, R. Guedes, and R. Santos, Double neutral Higgs production in the two-Higgs doublet model at the LHC, J. High Energy Phys. 08 (2009) 035; R. Grober and M. Muhlleitner, Composite Higgs boson pair production at the LHC, J. High Energy Phys. 06 (2011) 020; M. Gillioz, R. Grober, C. Grojean, M. Muhlleitner, and E. Salvioni, Higgs low-energy theorem (and its corrections) in composite models, J. High Energy Phys. 10 (2012) 004; C. Han, X. Ji, L. Wu, P. Wu, and J. M. Yang, Higgs pair production with SUSY QCD correction: Revisited under current experimental constraints, J. High Energy Phys. 04 (2014) 003; K. Nishiwaki, S. Niyogi, and A. Shivaji, ttH anomalous coupling in double Higgs production, J. High Energy Phys. 04 (2014) 011; J. M. No and M. Ramsey-Musolf, Probing the Higgs portal at the LHC through resonant di-Higgs production, Phys. Rev. D **89**, 095031 (2014); C. R. Chen and I. Low, Double take on new physics in double Higgs boson production, Phys. Rev. D **90**, 013018 (2014); B. Hespel, D. Lopez-Val, and E. Vryonidou, Higgs pair production via gluon fusion in the Two-Higgs-Doublet Model, J. High Energy Phys. 09 (2014) 124; B. Bhattacherjee and A. Choudhury, Role of supersymmetric heavy Higgs boson production in the self-coupling measurement of 125 GeV Higgs boson at the LHC, Phys. Rev. D **91**, 073015 (2015); V. Barger, L. L. Everett, C. B. Jackson, A. D. Peterson, and G. Shaughnessy, New Physics in Resonant Production of Higgs Boson Pairs, Phys. Rev. Lett. **114**, 011801 (2015); N. Liu, S. Hu, B. Yang, and J. Han, Impact of top-Higgs couplings on Di-Higgs production at future colliders, J. High Energy Phys. 01 (2015) 008; F. Goertz, A. Papaefstathiou, L. L. Yang, and J. Zurita, Higgs boson pair production in the $D=6$ extension of the SM, J. High Energy Phys. 04 (2015) 167; A. Papaefstathiou, Discovering Higgs boson pair production through rare final states at a 100 TeV collider, Phys. Rev. D **91**, 113016 (2015); R. Grober, M. Muhlleitner, M. Spira, and J. Streicher, NLO QCD corrections to Higgs pair production including dimension-6 operators, J. High Energy Phys. 09 (2015) 092; C. T. Lu, J. Chang, K. Cheung, and J. S. Lee, An exploratory study of Higgs-boson pair production, J. High Energy Phys. 08 (2015) 133; S. M. Etesami and M. Mohammadi Najafabadi, Double Higgs boson production with a jet substructure analysis to probe extra dimensions, Phys. Rev. D **92**, 073013 (2015); H. J. He, J. Ren, and W. Yao, Probing new physics of cubic Higgs boson interaction via Higgs pair production at hadron colliders, Phys. Rev. D **93**, 015003 (2016); Q. H. Cao, B. Yan, D. M. Zhang, and H. Zhang, Resolving the degeneracy in single Higgs production with Higgs pair production, Phys. Lett. B **752**, 285 (2016); Q. H. Cao, G. Li, B. Yan, D. M. Zhang, and H. Zhang, Double Higgs production at the 14 TeV LHC and a 100 TeV pp collider, Phys. Rev. D **96**, 095031 (2017); T. Corbett, A. Joglekar, H. L. Li, and J. H. Yu, Exploring extended scalar sectors with di-Higgs signals: A Higgs EFT perspective, J. High Energy Phys. 05 (2018) 061.

[15] G. Aad *et al.* (ATLAS Collaboration), Combination of searches for Higgs boson pairs in pp collisions at $\sqrt{s}=$ 13 TeV with the ATLAS detector, Phys. Lett. B **800**, 135103 (2020).

[16] A. M. Sirunyan *et al.* (CMS Collaboration), Combination of Searches for Higgs Boson Pair Production in Proton-Proton Collisions at $\sqrt{s}=13$ TeV, Phys. Rev. Lett. **122**, 121803 (2019).

[17] M. Cepeda *et al.*, Report from Working Group 2: Higgs physics at the HL-LHC and HE-LHC, CERN Yellow Rep. Monogr. **7**, 221 (2019).

[18] K. Fujii *et al.*, Physics case for the international linear collider, arXiv:1506.05992.

[19] J. Braathen and S. Kanemura, Leading two-loop corrections to the Higgs boson self-couplings in models with extended scalar sectors, Eur. Phys. J. C **80**, 227 (2020).

[20] J. Chang, K. Cheung, J. S. Lee, C. T. Lu, and J. Park, Higgs-boson-pair production $H(\to b\bar{b})H(\to \gamma\gamma)$ from gluon fusion at the HL-LHC and HL-100 TeV hadron collider, Phys. Rev. D **100**, 096001 (2019).

[21] J. Chang, K. Cheung, J. S. Lee, and J. Park, Probing the trilinear Higgs boson self-coupling at the high-luminosity LHC via multivariate analysis, Phys. Rev. D **101**, 016004 (2020).

[22] G. Heinrich, S. P. Jones, M. Kerner, G. Luisoni, and E. Vryonidou, NLO predictions for Higgs boson pair production with full top quark mass dependence matched to parton showers, J. High Energy Phys. 08 (2017) 088.

[23] G. Heinrich, S. P. Jones, M. Kerner, G. Luisoni, and L. Scyboz, Probing the trilinear Higgs boson coupling in di-Higgs production at NLO QCD including parton shower effects, J. High Energy Phys. 06 (2019) 066.

[24] M. Grazzini, G. Heinrich, S. Jones, S. Kallweit, M. Kerner, J. M. Lindert, and J. Mazzitelli, Higgs boson pair production at NNLO with top quark mass effects, J. High Energy Phys. 05 (2018) 059.

[25] L. B. Chen, H. T. Li, H. S. Shao, and J. Wang, Higgs boson pair production via gluon fusion at N^3LO in QCD, Phys. Lett. B **803**, 135292 (2020).L. B. Chen, H. T. Li, H. S. Shao, and J. Wang, The gluon-fusion production of Higgs boson pair: N^3LO QCD corrections and top-quark mass effects, J. High Energy Phys. 03 (2020) 072.

[26] P. Artoisenet, R. Frederix, O. Mattelaer, and R. Rietkerk, Automatic spin-entangled decays of heavy resonances in Monte Carlo simulations, J. High Energy Phys. 03 (2013) 015.

[27] R. Contino, D. Curtin, A. Katz, M. Mangano, G. Panico, M. Ramsey-Musolf, G. Zanderighi *et al.*, Physics at a 100 TeV pp collider: Higgs and EW symmetry breaking studies, CERN Yellow Rep. 255 (2017), https://doi.org/10.23731/CYRM-2017-003.255.

[28] S. Dulat, T.-J.Hou, J. Gao, M. Guzzi, J. Huston, P. Nadolsky, J. Pumplin, C. Schmidt, D. Stump, and C.-P. Yuan, New parton distribution functions from a global analysis of quantum chromodynamics, Phys. Rev. D **93**, 033006 (2016).

[29] M. L. Mangano, M. Moretti, F. Piccinini, and M. Treccani, Matching matrix elements and shower evolution for top-quark production in hadronic collisions, J. High Energy Phys. 01 (2007) 013.

[30] J. Alwall *et al.*, Comparative study of various algorithms for the merging of parton showers and matrix elements in hadronic, Eur. Phys. J. C **53**, 473 (2008).

[31] T. Sjöstrand, S. Ask, J. R. Christiansen, R. Corke, N. Desai, P. Ilten, S. Mrenna, S. Prestel, C. O. Rasmussen, and P. Z. Skands, An introduction to PYTHIA 8.2, Comput. Phys. Commun. **191**, 159 (2015).

[32] J. de Favereau, C. Delaere, P. Demin, A. Giammanco, V. Lemaître, A. Mertens, and M. Selvaggi (DELPHES 3 Collaboration), DELPHES 3, A modular framework for fast simulation of a generic collider experiment, J. High Energy Phys. 02 (2014) 057.

[33] J. Alwall, R. Frederix, S. Frixione, V. Hirschi, F. Maltoni, O. Mattelaer, H. S. Shao, T. Stelzer, P. Torrielli, and M. Zaro, The automated computation of tree-level and next-to-leading order differential cross sections, and their matching to parton shower simulations, J. High Energy Phys. 07 (2014) 079.

[34] A. Hoecker, P. Speckmayer, J. Stelzer, J. Therhaag, E. von Toerne, and H. Voss, TMVA: Toolkit for multivariate data analysis, *Proc. Sci.*, ACAT2007 (2007) 040.

[35] Rene Brun and Fons Rademakers, ROOT—An object oriented data analysis framework, Nucl. Instrum. Methods Phys. Res., Sect. A **389**, 81 (1997). See also [root.cern.ch/] (http://root.cern.ch/).

[36] G. Cowan, K. Cranmer, E. Gross, and O. Vitells, Asymptotic formulae for likelihood-based tests of new physics, Eur. Phys. J. C **71**, 1554 (2011).

[37] M. L. Mangano, G. Ortona, and M. Selvaggi, Measuring the Higgs self-coupling via Higgs-pair production at a 100 TeV p-p collider, arXiv:2004.03505.